Applied Catalysis B: Environmental 160–161 (2014) 240–246

Contents lists available at ScienceDirect

Applied Catalysis B: Environmental

journal homepage: www.elsevier.com/locate/apcatb

A new approach to prepare Ti^{3+} self-doped TiO_2 via $NaBH_4$ reduction and hydrochloric acid treatment

Wenzhang Fang[a], Mingyang Xing[a], Jinlong Zhang[a,b,*]

[a] Key Laboratory for Advanced Materials and Institute of Fine Chemicals, East China University of Science and Technology, 130 Meilong Road, Shanghai 200237, PR China
[b] Department of Chemistry, Tsinghua University, Beijing 100084, PR China

ARTICLE INFO

Article history:
Received 11 March 2014
Received in revised form 16 May 2014
Accepted 18 May 2014
Available online 27 May 2014

Keywords:
TiO_2 photocatalyst
Ti^{3+} doping
HCl washing treatment
$NaBH_4$ reductant
Photocatalytic mechanism

ABSTRACT

Ti^{3+} self-doped TiO_2 are successfully prepared via a simple one-step calcination method, by using low-cost $NaBH_4$ as the reductant. The as-prepared samples are characterized by different techniques such as X-ray diffraction (XRD), UV–vis diffuse reflectance spectroscopy (UV–vis DRS), Electron paramagnetic resonance (EPR), X-ray photoelectron spectroscopy (XPS), and Fourier transformation infrared spectroscopy (FTIR). EPR spectra confirm the presence of Ti^{3+} in the bulk of the samples rather than on the surface, which is the reason for the high photocatalytic performance of the catalyst under visible light irradiation. It is worth noting that the visible light absorption is enhanced after HCl washing, and the photocatalytic activity of Ti^{3+} self-doped TiO_2 is proportional to the concentration of the doped Ti^{3+}. Interestingly, the photocatalytic activity of the catalyst under UV light also increases after HCl washing treatment, which is caused by the increase of BET surface area.

1. Introduction

TiO_2 has been extensively studied since the discovery of its ability to produce H_2 from water [1]. Utilization of solar energy to produce hydrogen from water has been considered as the ultimate solution to the energy crisis for a long time. However, the band gap of 3.2 eV for anatase phase deeply limits its practical applications, that is, pure TiO_2 can only absorb wavelength less than 387 nm so that the visible light from solar energy cannot be well utilized. In order to enhance the photocatalytic activity of TiO_2, many studies have been done on band gap engineering. Cations such as Fe, V, La, Cr, Al, Ag and Mn were used as dopants to be introduced into the lattice of TiO_2 to reduce its bandgap [2–4]. Nonmetal doping was also used to improve the adsorption of TiO_2, such as N [5–8], C [9,10], and S [11] doping modifications. And there are also some other studies related to co-doped TiO_2 and tri-doped TiO_2 with transition metals and nonmetals [12–16]. However, the introduction of other impurity elements may result into thermal instability, expensive ion-implantation facility and more carrier recombination centers [6]. As a result, it will greatly hinder the photocatalytic efficiency of TiO_2 and limit its industrial production [17].

Recently, Ti^{3+} self-doped TiO_2 was reported to exhibit high visible light absorption and considerable photochemistry performance [17–22]. The reported methods to prepare Ti^{3+} doped TiO_2 include calcination under UHV atmosphere [23] or reducing conditions [24], UV irradiation [25,26], reducing treatment in situ [17], ion beam enhanced deposition [27] and plasma treatment [28]. Among these methods, the former three methods have attracted more attentions because of the simple chemical processes and low-cost facilities.

Zuo et al. reported a facile solution method to synthesize partially reduced rutile TiO_2 with active facets and Ti^{3+} presented in the bulk of the catalyst [29]. However, the concentration of Ti^{3+} could not be well controlled and the particle size was up to 500 nm, which might greatly inhibit its practical applications in a diverse set of solar energy systems. Despite the fact that reduced TiO_2 nanoparticles with enhanced visible absorption have triggered an explosion of interest, the study of Ti^{3+} doping is still far from satisfactory, and there are still lots of problems left to be solved in this area [18,20,24]. Relatively economic and simple techniques are required to obtain mass production of reduced TiO_2.

Recently, we successfully synthesized a series of TiO_2 catalysts self-doped with Ti^{3+} through a simple one-step solvo-thermal method [30], with low-cost $NaBH_4$ as the reductant. In this simple and economic method, HCl solution was demonstrated to be

* Corresponding authors at: East China University of Science and Technology, Key Lab for Advanced Materials and Institute of Fine Chemicals, 130 Meilong Road, Shanghai 200237, China. Tel.: +86 021 64252062; fax: +86 021 64252062.
E-mail addresses: mingyangxing@ecust.edu.cn (M. Xing), jlzhang@ecust.edu.cn (J. Zhang).

http://dx.doi.org/10.1016/j.apcatb.2014.05.031
0926-3373/

a useful reagent to remove the by-products especially the boron oxide species. But the carbonaceous impurities coated on the surface remained difficult to be wiped off. Although the HCl solution had a certain effect on removing the carbonaceous impurities, there was still a characteristic peak of C=O bond shown at 288.6 eV in C1s XPS characterization [30], indicating the presence of residual carbonaceous impurities. These impurities covered on the catalyst surface could significantly diminish the number of active sites and decrease the absorption intensity in the visible region [31–33].

In order to fully eliminate the negative effects of carbonaceous impurities, herein, we employ a simple one-step calcination method to introduce Ti^{3+} and oxygen vacancies into TiO_2 without introducing any other impurity elements. By using low-cost $NaBH_4$ as the reductant, Ti^{3+} is successfully introduced into the bulk of TiO_2, and its visible light photocatalytic activity is significantly enhanced as excepted. Interestingly, the HCl washing treatment greatly increases the BET surface area of prepared catalysts, which further improves the photocatalytic performance of TiO_2 under UV light irradiation.

2. Materials and methods

2.1. Preparation of Ti^{3+} self-doped TiO_2

5 mL tetrabutyl titanate (TBOT, C.P.) and 25 mL EtOH (A.R.) were mixed to obtain solution A while 4 mL HNO_3 (0.6 M) and 5 mL EtOH were mixed to obtain solution B. Under magnetic stirring conditions, solution B was dropwise added to solution A to form a sol. Then a certain amount of $NaBH_4$ (C.P.) was added into the sol until it reconstituted into a gel. The above mixture was transferred into a ceramic bowl and calcined for 180 min at 500 °C in the air to gain a series of TiO_2 nanoparticles, which were denoted as m-TiO_2, where "m" described the added amount of $NaBH_4$ (m = 0.025, 0.05, 0.1, 0.3 and 0.4 g). Pure-TiO_2 was prepared by the same method without $NaBH_4$.

For comparison, Ti^{3+} self-doped TiO_2 was synthesized by solvothermal method as previously reported [30].

2.2. HCl washing treatment

In a 150 mL pyrex beaker, 0.5 g m-TiO_2 nanoparticles were added into 100 mL HCl solution (1 M). After stirring for 6 h, the samples were washed by distilled water for several times and then dried at 60 °C in vacuum for 12 h.

2.3. Physical characterization of the catalysts

X-ray diffraction (XRD) analysis of the prepared photocatalysts was carried out at room temperature using Cu $K\alpha$ radiation (λ = 0.15406 nm) with a Rigaku Ultima IV apparatus equipped with a graphite monochromator. It is operated at 40 kV and 40 mA, and the diffraction patterns were recorded in the angular range of 10–80°.

X-ray photoelectron spectroscopy (XPS, Perkin-Elmer PHI 5000C ESCA system with Al Kα radiation) was operated at 250 W at room temperature. The shift of the binding energy scale caused by relative surface charging was corrected by referencing the C1s level at 284.6 eV.

The UV–vis absorbance spectra were obtained by referencing the $BaSO_4$ sample disk as the standard at room temperature in air. The disk samples were dry-pressed and detected with a Scan UV–vis spectrophotometer (Shimadzu, UV-2450) equipped with an integrating sphere assembly. The data was collected at the range of 200–800 nm.

The electron paramagnetic resonance (EPR) spectra were collected at room temperature on a Bruker EMX-8/2.7 EPR spectrometer.

Carbonaceous group vibrations were detected with KBr disks which contain the powder sample in the Fourier transform infrared (FTIR) spectrometer (Nicolet Magna 550).

BET surface area measurements were carried out by N_2 adsorption–desorption at 77 K using a Micromeritics ASAP2020 instrument. The samples were pre-dried at 300 °C in N_2.

2.4. Photocatalytic activities of Ti^{3+} self-doped TiO_2

The photodegradation of Rhodamine B (RhB) of the samples was carried out to evaluate the photocatalytic activities of different samples. In a 100 mL quartz photoreactor, 0.07 g photocatalyst was dispersed into 70 mL RhB (10 mg/L) solution, which was then stirred for 30 min in the dark in order to achieve the adsorption–desorption equilibrium. The mixture was subsequently irradiated under a 500 W tungsten halogen lamp equipped with a UV cut-off filter (λ > 420 nm) to simulate the photoreaction under visible light. As for UV light irradiation, a 300 W high-pressure Hg lamp was used with a UV-cut optical filter (λ < 365 nm). In order to maintain a stable ambient temperature during the photocatalytic process, the lamp was placed into a quartz jacket with flowing water around it. Finally, the samples were taken from the mixture solution every given time interval, centrifuged to remove the precipitate, and then analyzed by the UV–vis spectrophotometer (Shimadzu, UV-2450).

3. Results and discussion

3.1. Characterization of Ti^{3+} self-doped TiO_2

The XRD patterns of the prepared samples before HCl treatment are shown in Fig. 1a. It can be found that most of the diffraction peaks of the catalysts are ascribed to the anatase phase. However, as the amount of $NaBH_4$ increases, peaks corresponding to tincalconite ($Na_2B_4O_7{\cdot}5H_2O$, PDF 07-0277) and sodium titanium oxide ($Na_{0.23}TiO_2$, PDF 22-1404) arise obviously. After HCl washing (as shown in Fig. 1b), peaks of tincalconite disappear because of its instability in acid. These observations indicate that tincalconite may be washed out during the HCl washing treatment. In addition, it is notable that peaks of rutile phase are found in the XRD pattern of pure-TiO_2 but not shown in the case of Ti^{3+} self-doped TiO_2. The inhibition of the phase transformation may be caused by the self-doping of Ti^{3+} and production of oxygen defects.

The crystallite sizes are determined from the Scherrer equation:

$$D = \frac{K\lambda}{\beta \cos\theta} \quad (1)$$

where K = 0.89 is shape factor, λ is the wavelength of X-ray irradiation (Cu $K\alpha$ = 0.154056 nm), β is the full-width half-maximum (FWHM) of the diffraction peak and θ is the X-ray diffraction angle. The result is listed in Table 1.

Table 1
Structural characteristics of various samples.

Samples	Before washing		After washing	
	Particle sizes (nm)	d-spacing (Å)	Particle sizes (nm)	d-spacing (Å)
Pure-TiO_2	35.6	3.5	35.6	3.5
0.025-TiO_2	20.2	3.5	20.9	3.5
0.1-TiO_2	18.0	3.5	17.2	3.5
0.3-TiO_2	13.9	3.5	15.2	3.5
0.4-TiO_2	9.4	3.5	13.2	3.5

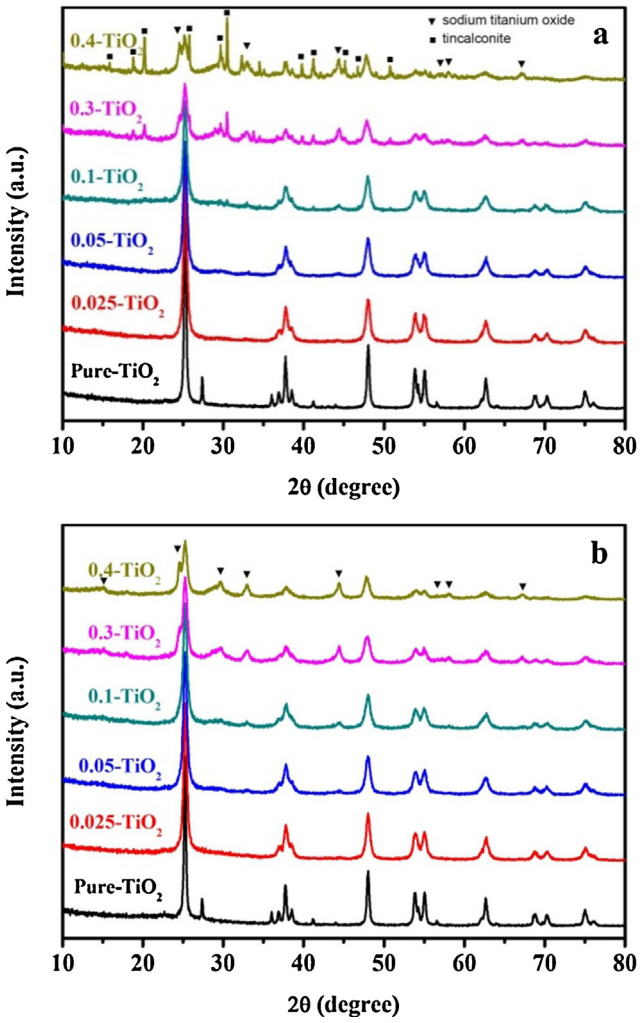

Fig. 1. XRD patterns of samples reduced by different amount of $NaBH_4$ before (a) and after HCl washing (b).

As shown in Table 1, the particle size of the catalysts decreases distinctly with the increasing amount of $NaBH_4$, owing to the inhibition of the growth of TiO_2 seeds caused by the impurities. During the calcination process, some by-products are produced when Ti^{4+} is reduced (Eq. (2)). However, the "*d*" space value does not change in Table 1, implying that the Ti^{3+} self-doping is not likely to change the unit cell dimension of reduced TiO_2. In addition, the particle sizes of various samples show little change after HCl washing.

Electron paramagnetic resonance (EPR) spectra are also recorded to detect the generation of Ti^{3+} in these samples. It has been reported that paramagnetic Ti^{3+} has a *g*-value of 1.94–1.99 and oxygen vacancy at $g = 2.004$ [28]. Two peaks are found at $g = 2.00$ and 1.98 corresponding to oxygen vacancy and Ti^{3+}, respectively, as shown in Fig. 2. As is known to all, the surface Ti^{3+} is not stable under illumination in air or water and it is easy to be oxidized by the oxygen, which will show an EPR signal at $g = 2.02$ corresponding to O^{2-} [17,34,35]. So the absence of such a peak in Fig. 2 indicates that Ti^{3+} presents in the bulk of TiO_2 rather than on the surface, which accounts for its high stability in air or water. With increasing amount of $NaBH_4$ added into the system, the sample of 0.1-TiO_2 shows the highest Ti^{3+} doping concentrations. In the calcination process, more $NaBH_4$ means more impurities like boron oxide species left on the surface of prepared samples, which will have a negative influence on the interaction between Ti^{4+} and the reducing species, causing the reduction of the concentration of Ti^{3+}

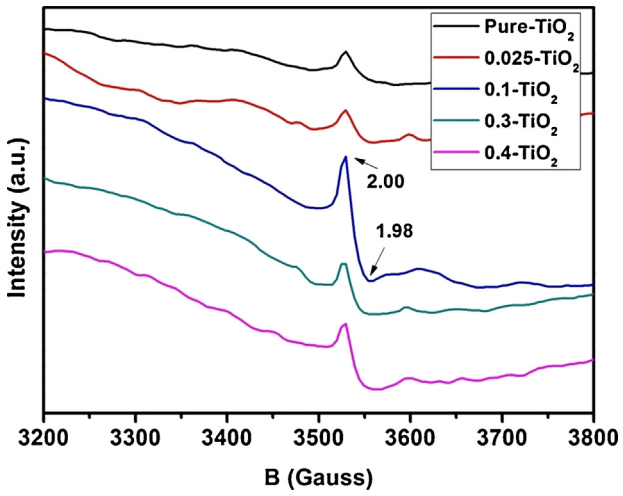

Fig. 2. EPR spectra of samples after HCl washing.

produced in the reaction [30]. As a result, adding excessive amounts of $NaBH_4$ during the preparation can decrease the concentration of Ti^{3+}.

3.2. The $NaBH_4$ reduction process

Ti^{3+} doped TiO_2, or reduced TiO_2 (TiO_{2-x}), has been demonstrated to exhibit visible light absorption [36]. Wang et al. [37] have reported that annealing the pristine TiO_2 nanowires in hydrogen atmosphere improves the performance for photoelectrochemical (PEC) water splitting. In the reducing atmosphere, Ti^{3+} can be easily obtained by the reduction of Ti^{4+}, along with the generation of oxygen vacancy sites which will produce donor states just below the conduction band [18]. In our method, hydrogen generation is achieved from the hydrolysis of sodium borohydride, as shown in the following equation:

$$8\,Ti^{4+} + NaBH_4 + 2\,H_2O \rightarrow 8\,Ti^{3+} + NaBO_2 + 8\,H^+ \quad (2)$$

This reaction is easy to realize, especially at high temperature and pressure. However, during the reduction process, a large number of boron oxide species are produced and absorbed on the surface of TiO_2 because of their insolubility in the ethanol. Fig. 3 shows the B1s XPS spectra of 0.1-TiO_2 before and after HCl washing. An absence of the characteristic peak at 187.5 eV corresponding

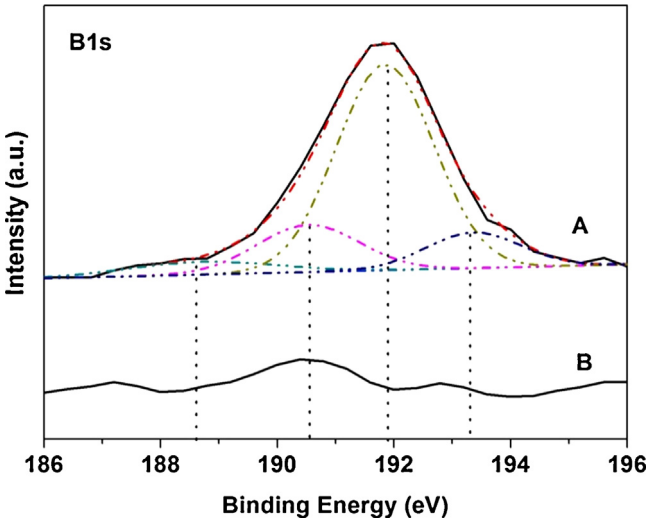

Fig. 3. B1s XPS spectra of 0.1-TiO_2 before (A) and after (B) HCl washing.

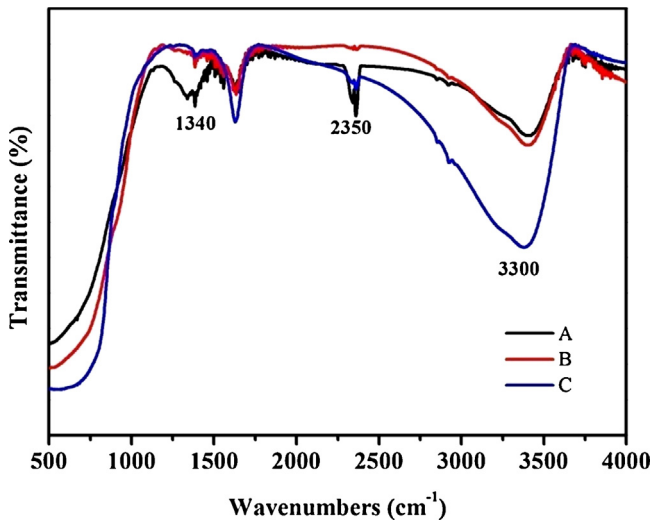

Fig. 4. FT-IR spectra of various samples: 0.1-TiO_2 before (A) and after (B) HCl washing; sample C prepared by our previous method (C).

to Ti–B proves that boron is not doped into the lattice of TiO_2 during the reduction process [38]. However, the peaks at 188.6 and 190.6 eV corresponding to residual $NaBH_4$ and BN arose during the calcination process. Other peaks are also observed at 191.8 and 193.2 eV, ascribing to the $Na_3B_3O_6$ and B_2O_3, respectively. After washing by HCl, the characteristic peak of boron oxide species ($Na_3B_3O_6$ and B_2O_3) are all weakened, as shown in Fig. 3, indicating that the by-product boron oxide species can be washed away by HCl solution.

Except some boron oxide species, there are also some residual carbonaceous impurities covering on the surface of the catalyst during the reduction process. FT-IR spectra of 0.1-TiO_2 before and after HCl washing and the sample prepared by our previous method are shown in Fig. 4. The peaks at 1340 cm^{-1} and 2350 cm^{-1} can be ascribed to gaseous CO_2 in air [39,40]. Compared with the Ti^{3+} self-doped TiO_2 prepared by the hydrothermal method in our previous report [30], the Ti^{3+} self-doped TiO_2 synthesized by calcination method is beneficial to the elimination of carbon impurities, especially the saturated and unsaturated carbon impurities, whose characteristic peaks at 2700–3300 cm^{-1} has a significant reduction.

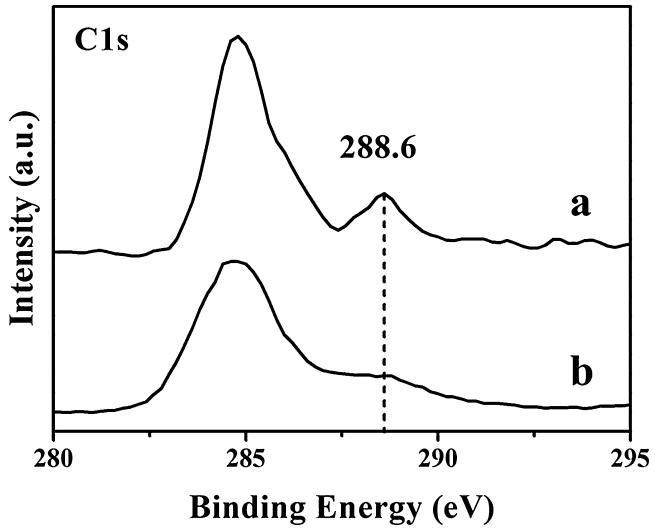

Fig. 5. C1s XPS spectra of various samples: the sample reported in our previous report (a) and 0.1-TiO_2 before HCl washing (b).

C1s XPS spectra (shown in Fig. 5) of 0.1-TiO_2 and the sample of Ti^{3+} doped TiO_2 reported in our previous work [30] before HCl washing are also given to detect the contents of carbon impurities. The boron oxide produced during the preparation can be easily washed out by HCl washing treatment. However, the carbonaceous impurities covered on the surface of the catalyst synthesized by hydrothermal method cannot be entirely washed away by the HCl solution, which shows a characteristic peak of C=O and COO at 288.6 eV in the C1s XPS spectra (Fig. 5, line a). In contrast, traditional carbon doped TiO_2 with enhanced photocatalytic activities shows characteristic peaks in lower binding energy [31,32]. And it is also reported that the surface coke carbons rather than the carbonate species are responsible for the visible light response [33]. As a result, the carbonaceous impurities covered on the surface of the catalysts dramatically diminish the number of active sites, which may make a negative effect on the sorption intensity in the visible region. In this system, the catalyst prepared by calcination method (Fig. 5, line b) shows less carbonaceous impurities compared with the one prepared by the hydrothermal method, indicating the superiority of the calcination method in significant elimination of the carbonaceous impurities.

Since calcination method is easy to burn off the surface carbonaceous impurities compared with the hydrothermal method [30], the weak absorption in visible light before HCl washing as shown in Fig. 6a is mainly caused by the boron oxide species coated on the surface of TiO_2, resulting in the shading of visible light irradiation on the catalyst, as shown in Eq. (2). Fig. 6b shows the UV-DRS spectra of different samples after HCl washing. It indicates that the absorption intensities of all the reduced TiO_2 are changing to be much stronger after the acid treatment. It is widely accepted that Ti^{3+} doping and presence of oxygen vacancies can lead to the formation of color center, which results into enhanced visible-light response [24,35]. Among all the catalysts reduced by $NaBH_4$ after washing, 0.1-TiO_2 shows strong absorbance in the visible-light region. As obtained by estimating the tangent in Fig. 6c, the band gap of 0.1-TiO_2 turns out to remain unchanged after the washing process (2.87 eV). To sum up, it can be predicted that during the washing treatment, the impurities tend to be washed away and the self-doped Ti^{3+} becomes much easier to be exposed. Hence, the elimination of surface boron oxide species by HCl treatment can expose more color centers introduced by Ti^{3+} and oxygen vacancies [39], leading to the improvement of absorption intensities in visible light region, as shown in Fig. 6a and b.

Oxygen vacancies are usually produced with the generation of Ti^{3+} during the preparation process. O1s XPS spectra of various samples before and after HCl washing are shown in Fig. 7. The peaks at 529.8 and 531.8 eV are ascribed to Ti—O bond and oxygen vacancy neighboring to Ti^{3+}, respectively [35]. The figure shows that the O_v intensity of 0.1-TiO_2 increases significantly after washing while that of pure TiO_2 stays still (Fig. 7a and b). After HCl washing, the O_v of 0.1-TiO_2 also shows higher intensity comparing to that of pure TiO_2 (Fig. 7c), which may indicate the huge inference of $NaBH_4$ reduction and HCl abstersion. It can be predicated that during the $NaBH_4$ reduction process, Ti^{3+} and oxygen vacancies might be easily covered by some boron oxide species as soon as they are produced, which will greatly inhibit the visible light absorption. Fortunately, HCl solution can successfully remove the surface impurities and expose the color centers on the surface of the catalyst. As a result, solar energy with longer wavelengths can directly reach the donor states just below the conduction band without any loss caused by the impurities covering [18,24].

3.3. Photocatalytic activities of Ti^{3+} self-doped TiO_2

We have employed the degradation of RhB on the as-prepared TiO_2 under visible light irradiation to explore the effect of Ti^{3+}

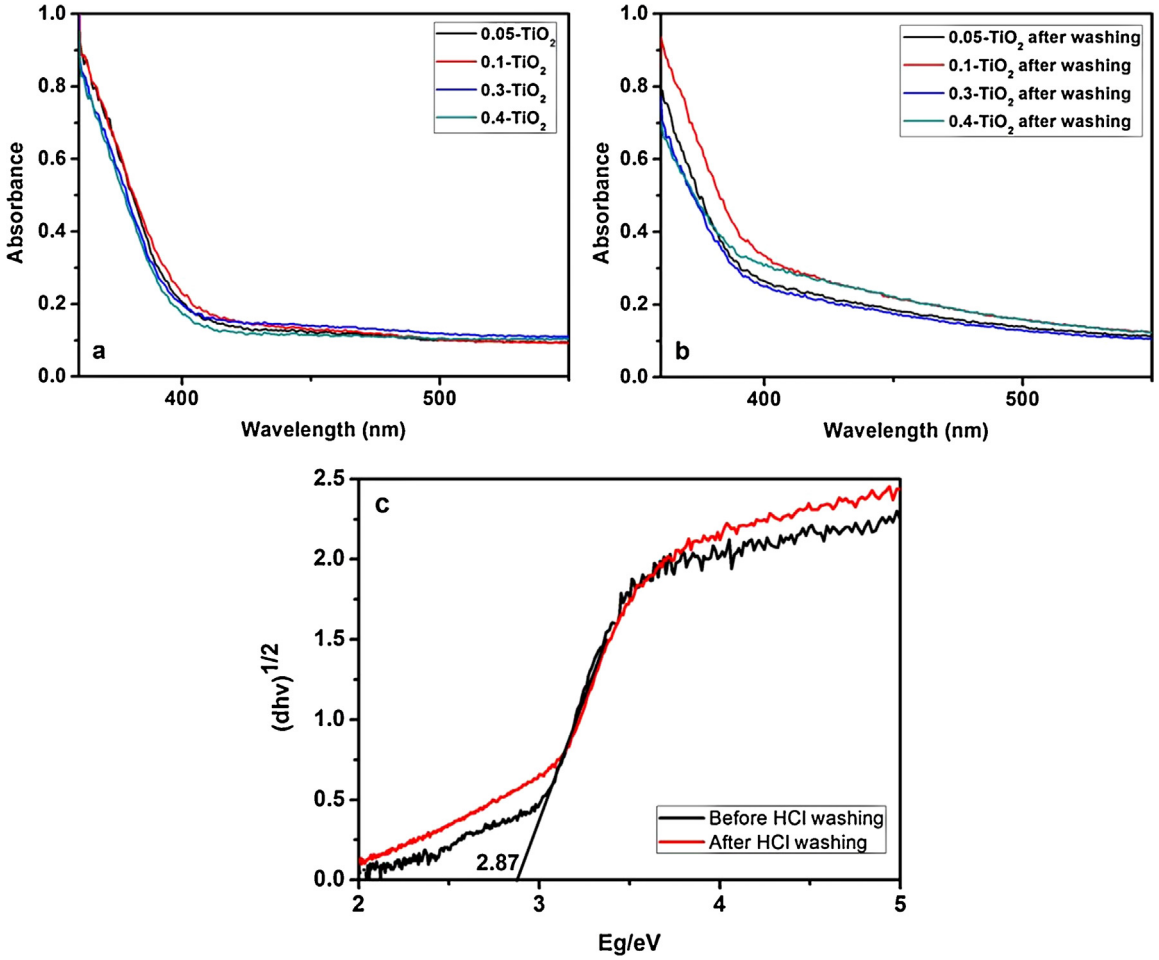

Fig. 6. UV–vis diffuse reflectance spectra of the samples before (a) and after (b) HCl washing; plot of transformed Kubelka–Munk function against the photon energy for the sample 0.1-TiO_2 (c).

self-doping modification. As shown in Fig. 8, after HCl treatment, the catalyst of 0.1-TiO_2 shows the highest visible-light photodegradation activity, resulting from its highest Ti^{3+} concentration among these samples, as shown in Fig. 2. From these two figures, it can be demonstrated that the photocatalytic activity of Ti^{3+} self-doped TiO_2 is proportional to the concentration of the doped Ti^{3+} in the catalyst, which is also dependence on the visible light wavelength absorption (Fig. 6b). While for traditional metal and nonmetal doping modification, excessive doping is likely to introduce a lot of carrier recombination centers, which will greatly decrease the photocatalytic activity of TiO_2 [5,14]. In order to investigate the stability of our catalysts, we also carried out the cycling degradation of RhB over the sample of 0.1-TiO_2 after washing treatment (Fig. 9). The result demonstrates the stable photocatalytic activity of our sample during the cycling process.

While illuminated by visible light, the photoelectron is excited to the impurity level introduced by the Ti^{3+} doping. As we reported before [35], this level existed in the form of $[O_v{\cdot}Ti^{3+}]^+$ can prolong the conduction life of photo-induced electron and hinder the recombination of the electron and hole [41], resulting in enhanced photocatalytic activities of the reduced TiO_2. The proposed mechanism of the self-doping of TiO_2 is illustrated in Scheme 1.

It can be found in Fig. 8 that the prepared catalysts after HCl washing show higher visible-light photocatalytic activities than before. In order to investigate the enhancement of the photocatalytic performance of our materials after washing, the rate constant of the photocatalytic degradation is obtained by pseudo-first order fit. As shown in Fig. 10, the degradation rate of 0.1-TiO_2 increases by 9 times from 1.57×10^{-3} to 14.29×10^{-3} min^{-1} after washing, owning to the removal of boron oxide species induced by the alcoholysis of TBOT on the surface of catalysts.

Although it has been reported that Ti^{3+} doping itself does not affect the UV-light photoactivity of TiO_2 [30], we also test the UV light degradation of RhB by Ti^{3+} self-doped TiO_2, as shown in Fig. 11. The Ti^{3+} self-doped TiO_2 catalysts present higher degradation rate than the pure TiO_2. This phenomenon can be ascribed to the decreasing of the particle sizes caused by impurity coating. Before HCl washing treatment, although the particle sizes of the Ti^{3+}-doped TiO_2 catalysts decrease with increasing amount of $NaBH_4$, the photodegradation rate does not increase because of the by-product boron oxide impurities coating on the surface reactive center. After washing treatment, the impurities are washed off and all the catalysts present enhanced photocatalytic activities. And the degradation rate turns to be higher under UV light irradiation with an increase in the amount of $NaBH_4$ caused by the particle size decreasing (Table 1).

In order to further confirm our suspect, the BET surface areas of various samples are presented in Table 2. As the measured structural characteristics show in Table 1, before HCl washing, there is no linear relationship between the particle size and the BET surface area. By washing treatment, the particle size of Ti^{3+} doped TiO_2 decreases but the BET surface area gradually increases with the increasing amount of NBH_4, owing to the removal of the by-product. It is worth noting that the photocatalytic activities of Ti^{3+} self-doped TiO_2 under UV light irradiation are always consistent with their BET surface areas either before or after HCl washing. It

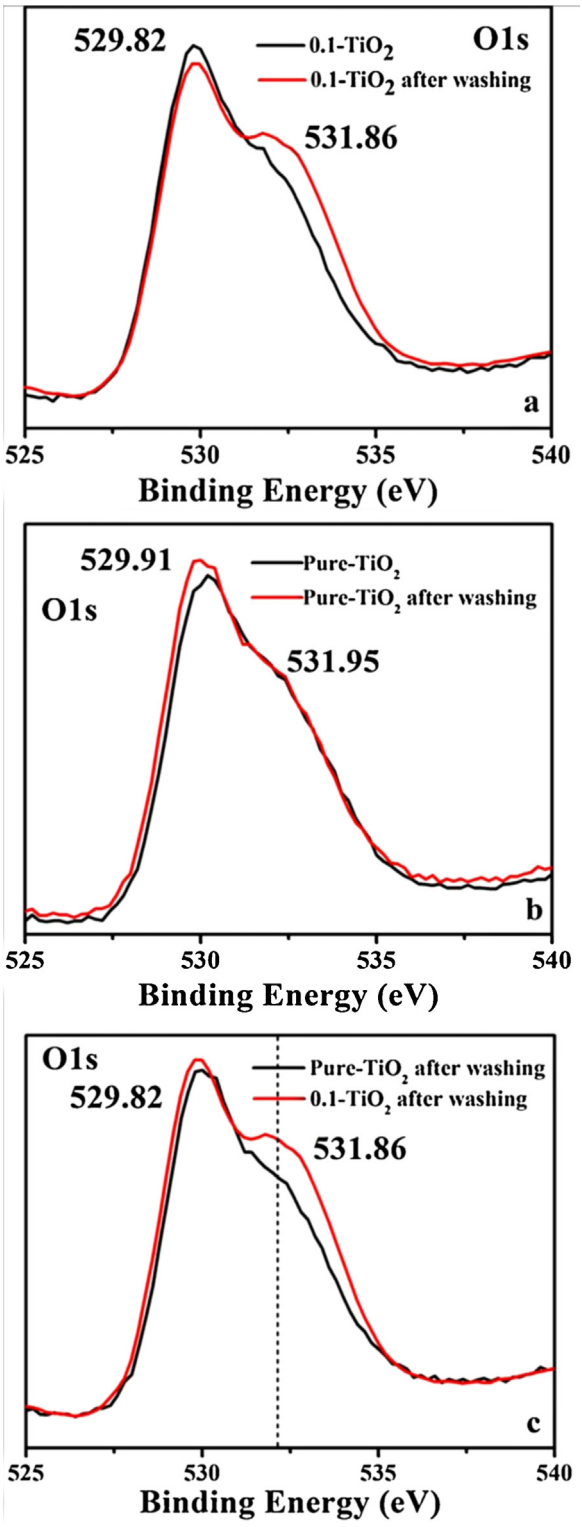

Fig. 7. O1s XPS spectra of the reduced samples: 0.1-TiO_2 before and after HCl washing (a); Pure TiO_2 before and after HCl washing (b); Pure TiO_2 and 0.1-TiO_2 after HCl washing (c).

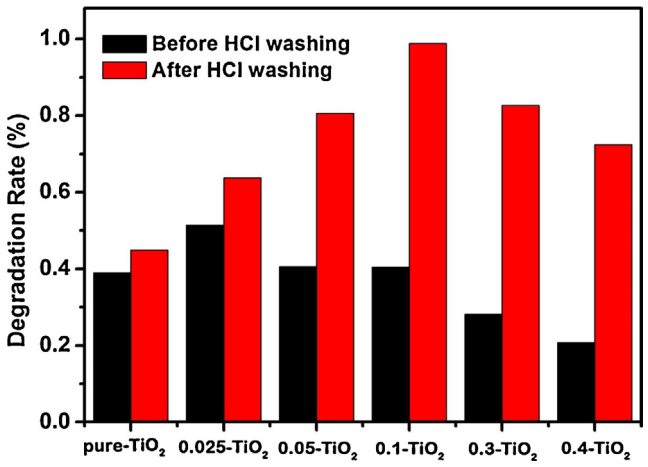

Fig. 8. Fractional removal of RhB of these samples after visible light irradiation for 5 h.

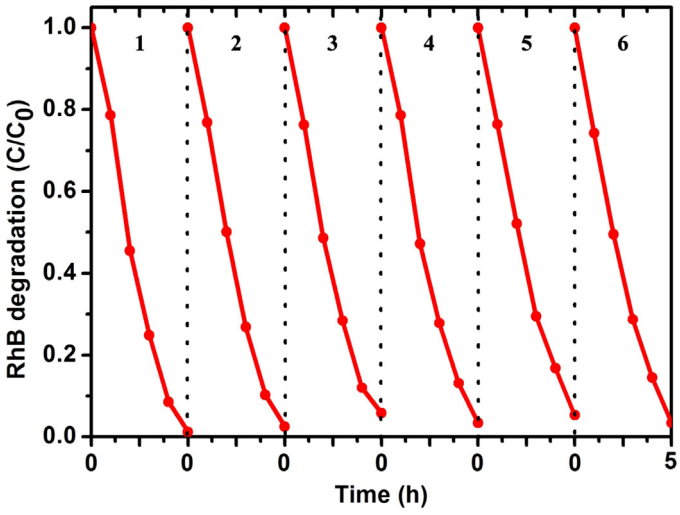

Fig. 9. Cycling degradation of RhB under visible light irradiation over the sample of 0.1-TiO_2 after washing.

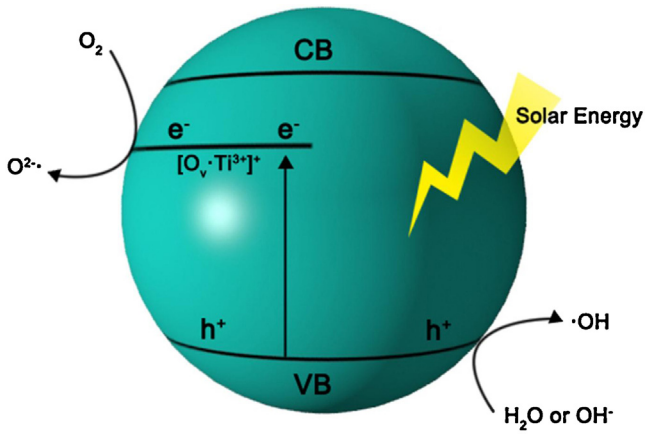

Scheme 1. Proposed mechanism of the self-doping of TiO_2.

can be concluded that the BET surface area plays a more important role in the UV-light photocatalytic activity because massive photogenerated electrons and holes are presented under the UV light irradiation. It was also found that the BET surface area of each Ti^{3+} self-doped TiO_2 sample increases after HCl treatment. As to sample 0.4-TiO_2, before HCl washing, there are massive boron oxide species covering on the surface of TiO_2. As a result, it presents a low-value BET surface area of the catalyst due to the space between particles filling by residual impurities [42]. After washing, the impurities unfavorable to the light absorption are removed, and the BET surface area arises obviously, accounting for the enhanced photocatalytic performance under UV light irradiation.

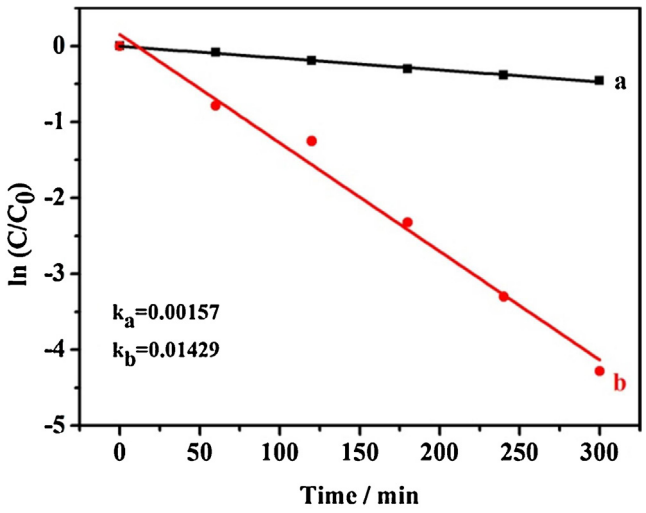

Fig. 10. Photocatalytic degradation of RhB by 0.1-TiO_2 before (a) and after (b) HCl washing under visible light irradiation represented by pseudo-first order fit.

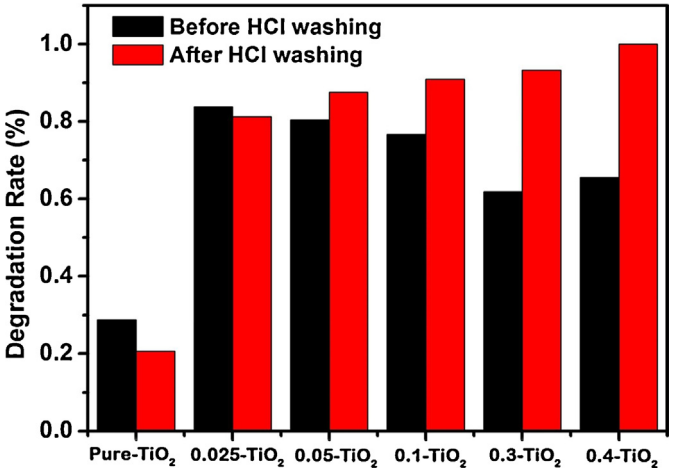

Fig. 11. Fractional removal of RhB after UV light irradiation for 40 min on the samples before and after HCl washing.

Table 2
BET surface area of various samples.

Samples	BET surface area (m^2/g) before HCl washing	BET surface area (m^2/g) after HCl washing
Pure-TiO_2	2.0	5.4
0.025-TiO_2	22.1	31.0
0.05-TiO_2	27.2	42.5
0.1-TiO_2	27.2	54.4
0.3-TiO_2	18.2	67.0
0.4-TiO_2	19.5	79.3

4. Conclusions

In summary, we employed a new approach to synthesize a series of Ti^{3+} self-doped TiO_2 via a simple one-step calcination method, by using $NaBH_4$ as the reductant. Calcination method is beneficial to burn off the carbon impurities, and HCl solution is used to wash out the by-product boron oxide coated on the surface of the catalysts. The Ti^{3+} generation is responsible for enhanced visible light absorption and photocatalytic activity, while particle size and BET surface area play a greater important role in the photocatalytic performance under UV light irradiation.

Acknowledgments

This work has been supported by the National Natural Science Foundation of China (21173077, 21377038, 21203062 and 21237003); the National Basic Research Program of China (973 Program, 2013CB632403), the Project of International Cooperation of the Ministry of Science and Technology of the People's Republic of China (No. 2011DFA50530); Science and Technology Commission of Shanghai Municipality (12230705000, 12XD1402200); the Research Fund for the Doctoral Program of Higher Education (20120074130001) and the Fundamental Research Funds for the Central Universities.

References

[1] A. Fujishima, K. Honda, Nature 238 (1972) 37–38.
[2] I. Justicia, P. Ordejón, G. Canto, J.L. Mozos, J. Fraxedas, G.A. Battiston, R. Gerbasi, A. Figueras, Adv. Mater. 14 (2002) 1399–1402.
[3] W. Choi, A. Termin, M.R. Hoffmann, J. Phys. Chem. 98 (1994) 13669–13679.
[4] M. Xing, D. Qi, J. Zhang, F. Chen, Chem. Eur. J. 17 (2011) 11432–11436.
[5] Y. Cong, J. Zhang, F. Chen, M. Anpo, J. Phys. Chem. C 111 (2007) 6976–6982.
[6] R. Asahi, T. Morikawa, T. Ohwaki, K. Aoki, Y. Taga, Science 293 (2001) 269–271.
[7] M. Xing, J. Zhang, F. Chen, Appl. Catal., B: Environ. 89 (2009) 563–569.
[8] M. Xing, W. Li, Y. Wu, J. Zhang, X. Gong, J. Phys. Chem. C 115 (2011) 7858–7865.
[9] S. Sakthivel, H. Kisch, Angew. Chem. Int. Ed. 42 (2003) 4908–4911.
[10] L. Zhao, X. Chen, X. Wang, Y. Zhang, W. Wei, Y. Sun, M. Antonietti, M.-M. Titirici, Adv. Mater. 22 (2010) 3317–3321.
[11] P. Xu, T. Xu, J. Lu, S. Gao, N.S. Hosmane, B. Huang, Y. Dai, Y. Wang, Energy Environ. Sci. 3 (2010) 1128–1134.
[12] J. Zhang, Y. Wu, M. Xing, S.A.K. Leghari, S. Sajjad, Energy Environ. Sci. 3 (2010) 715–726.
[13] M. Takeuchi, M. Matsuoka, M. Anpo, Res. Chem. Intermed. 38 (2012) 1261–1277.
[14] M. Xing, Y. Wu, J. Zhang, F. Chen, Nanoscale 2 (2010) 1233–1239.
[15] Y. Cong, J. Zhang, F. Chen, M. Anpo, D. He, J. Phys. Chem. C 111 (2007) 10618–10623.
[16] F. Dong, W. Zhao, Z. Wu, Nanotechnology 19 (2008) 365607.
[17] F. Zuo, L. Wang, T. Wu, Z. Zhang, D. Borchardt, P. Feng, J. Am. Chem. Soc. 132 (2010) 11856–11857.
[18] X. Chen, L. Liu, P.Y. Yu, S.S. Mao, Science 331 (2011) 746–750.
[19] C.S. Chen, T.C. Chen, C.C. Chen, Y.T. Lai, J.H. You, T.M. Chou, C.H. Chen, J.-F. Lee, Langmuir 28 (2012) 9996–10006.
[20] X. Chen, L. Liu, Z. Liu, M.A. Marcus, W.-C. Wang, N.A. Oyler, M.E. Grass, B. Mao, P.-A. Glans, P.Y. Yu, J. Guo, S.S. Mao, Sci. Rep. 3 (2013), http://dx.doi.org/10.1038/srep01510, Article no.: 1510.
[21] Z. Zheng, B. Huang, X. Meng, J. Wang, S. Wang, Z. Lou, Z. Wang, X. Qin, X. Zhang, Y. Dai, Chem. Commun. 49 (2013) 868–887.
[22] X. Liu, S. Gao, H. Xu, Z. Lou, W. Wang, B. Huang, Y. Dai, Nanoscale 5 (2013) 1870–1875.
[23] G. Lu, A. Linsebigler, J.T. Yates, J. Phys. Chem. 98 (1994) 11733–11738.
[24] S. Hoang, S.P. Berglund, N.T. Hahn, A.J. Bard, C.B. Mullins, J. Am. Chem. Soc. 134 (2012) 3659–3662.
[25] S. Mezhenny, P. Maksymovych, T.L. Thompson, O. Diwald, D. Stahl, S.D. Walck, J.T. Yates Jr., Chem. Phys. Lett. 369 (2003) 152–158.
[26] T.L. Thompson, J.T. Yates, Chem. Rev. 106 (2006) 4428–4453.
[27] F. Zhang, S. Jin, Y. Mao, Z. Zheng, Y. Chen, X. Liu, Thin Solid Films 310 (1997) 29–33.
[28] I. Nakamura, N. Negishi, S. Kutsuna, T. Ihara, S. Sugihara, K. Takeuchi, J. Mol. Catal. A: Chem. 161 (2000) 205–212.
[29] F. Zuo, K. Bozhilov, R.J. Dillon, L. Wang, P. Smith, X. Zhao, C. Bardeen, P. Feng, Angew. Chem. 124 (2012) 6327–6330.
[30] M. Xing, W. Fang, M. Nasir, Y. Ma, J. Zhang, M. Anpo, J. Catal. 297 (2013) 236–243.
[31] X. Chen, C. Burda, J. Am. Chem. Soc. 130 (2008) 5018–5019.
[32] H. Irie, Y. Watanabe, K. Hashimoto, Chem. Lett. 32 (2003) 772–773.
[33] Y. Wu, M. Xing, J. Zhang, J. Hazard. Mater. 192 (2011) 368–373.
[34] M. Anpo, M. Che, B. Fubini, E. Garrone, E. Giamello, M. Paganini, Top. Catal. 8 (1999) 189–198.
[35] M. Xing, J. Zhang, F. Chen, B. Tian, Chem. Commun. 47 (2011) 4947–4949.
[36] R. Sasikala, A. Shirole, V. Sudarsan, T. Sakuntala, C. Sudakar, R. Naik, S.R. Bharadwaj, Int. J. Hydrogen Energy 34 (2009) 3621–3630.
[37] G. Wang, H. Wang, Y. Ling, Y. Tang, X. Yang, R.C. Fitzmorris, C. Wang, J.Z. Zhang, Y. Li, Nano Lett. 11 (2011) 3026–3033.
[38] Y. Wu, M. Xing, J. Zhang, F. Chen, Appl. Catal., B: Environ. 97 (2010) 182–189.
[39] T. Sekiya, K. Ichimura, M. Igarashi, S. Kurita, J. Phys. Chem. Solids 61 (2000) 1237–1242.
[40] E. Finocchio, C. Cristiani, G. Dotelli, P.G. Stampino, L. Zampori, Vib. Spectrosc. 71 (2014) 47–56.
[41] M. Sugawara, Phys. Rev. B: Condens. Matter 51 (1995) 10743–10754.
[42] D. Mao, G. Lu, Q. Chen, Z. Xie, Y. Zhang, Catal. Lett. 77 (2001) 119–124.